14th IEA Heat Pump Conference
15-18 May 2023, Chicago, Illinois

Boiling Heat Transfer of Ammonia in a Flooded Evaporator of Adsorption Heat Pumps

Jin Sub Kim[a,*], Dong Hwan Shin[a], Wookyoung Kim[a] and Seok Ho Yoon[a]

[a]Department of Thermal Energy Solutions, Korea Institute of Machinery and Materials, Daejeon, 34103, Republic of Korea

Abstract

Adsorption heat pumps can provide process heat to the industry by converting wasted heat from the plants to more useful heat of high temperature. Ammonia is suitable for a working fluid of the adsorption heat pump for decarbonization since it has zero global warming potential (GWP) and ozone depletion potential (ODP). Thermal performance of the ammonia adsorption heat pump is closely related to the boiling heat transfer in a flooded evaporator of the heat pump. Boiling heat transfer of ammonia on the plain stainless steel tube with an outer diameter of 15.87 mm was investigated at three different saturation pressures of 6.15, 8.57, and 11.7 bar (corresponding saturation temperatures of 10, 20, and 30 ℃). Considerable hysteresis between increasing heat flux and decreasing heat flux cases was observed. Measured boiling heat transfer coefficients were compared with previous correlations, and Stephan-Abdelsalam's correlation showed best agreement with the measurement. Boiling heat transfer on the enhanced tube with low fins was also examined, which exhibited large enhancement of the boiling heat transfer coefficient.

Keywords: Adsorption heat pump; Ammonia; Pool boiling; Flooded evaporator; Hysteresis

1. Introduction

The decarbonization of thermal energy associated with building and industry sectors is essential for attaining the 2050 Net-zero goal. Thermally driven heat pumps such as absorption and adsorption heat pumps are regarded as one of the key technologies improving the energy efficiency in heating and cooling section, and eventually replacing conventional fossil fuels [1]. An adsorption heat pump can be operated with lower grade waste heat and is free from greenhouse gas emission because it utilizes natural refrigerants like water and ammonia [2]. Although ammonia is toxic and flammable, it has lots of advantages of high latent heat, chemical stability, and higher operating pressure above atmosphere [1].

Numerous previous studies have revealed basic heat transfer characteristics of ammonia in the heat exchange devices such as boiler and flooded evaporator. Spindler [3] thoroughly reviewed pool boiling heat transfer data of ammonia and compared them with general pool boiling correlations. Experimental data include pool boiling on a single tube [4], heat transfer enhancement techniques [5-6], boiling phenomena on tube bundles [7], and spray evaporation [8]. Zheng et al. [9] investigated the effect of lubricant oil on shell-side boiling heat transfer coefficient and concluded that the heat transfer coefficient first decreased with increasing oil concentration, then increased with a further increase in concentration. Abbas et al. [10] also reviewed various empirical correlations for outside boiling on single tube and bundles in ammonia. They concluded that existing correlations are to be cautiously applied because there is a wide disparity among them. Fernandez-Seara et al. [11] compared the heat transfer coefficient of spray evaporation with that of pool boiling on a horizontal plain tube in ammonia. They also showed boiling heat transfer improvement on an integral finned tube in a flooded evaporator [12]. They reported that a large hysteresis between increasing heat flux and decreasing heat flux was initially observed but diminished as the time passed (10 hours).

* Corresponding author. Tel.: +82-42-868-7807; fax: +82-42-868-7338.
E-mail address: jskim129@kimm.re.kr.

Despite abovementioned previous studies, there are still lots of unresolved phenomena about pool boiling of ammonia in a flooded evaporator. More elaborate investigation is required to understand the complicated phenomena of ammonia including boiling incipience, hysteresis, and effect of surface structures in the flooded evaporator. The present study is aimed to investigate the hysteresis in boiling curves of ammonia and to clarify the effect of low fin structure on boiling performance, and to compare the measured data with previous correlations.

2. Experimental Setup

2.1. Experimental apparatus

The test chamber was made of stainless steel with a wall thickness of 6.5 mm to withstand an internal pressure as high as 20 bar, which corresponds to the saturation pressure of ammonia at 49.4 ℃. The length of the test chamber is 796 mm, and the internal diameter is 254.4 mm. The chamber is filled with ammonia, and the liquid level of the ammonia pool reaches approximately to the center of the chamber. The test tube was located at the bottom-center of the liquid pool as shown in Fig. 1. The test tube was likewise made of stainless steel with an outer diameter of 15.87 mm, and the inner diameter was 13.39 mm. Smooth tube and enhanced tube were prepared to investigate the effect of surface geometry on boiling heat transfer performance. Important geometric parameters are designated in Fig. 2 and corresponding values for smooth and enhanced (low fin) tubes are tabulated in Table 1. A smooth tube has machine-roughened surface, whose arithmetic average roughness (R_a) was measured as 0.296 μm using the surface roughness tester. The enhanced tube has low fins with a height of 1.33 mm. The fin pitch was 0.977 mm (26 fins per inch), and wall thickness (t_w) was 0.63 mm. Since the tube was compressed by the fin rolling machine during the fabrication process, the outer and inner diameters of the enhanced tube were reduced to 13.07 mm and 11.81 mm, respectively. The outmost diameter including low fins was maintained to be 15.73 mm, which is nearly the same as the outer diameter of the smooth tube.

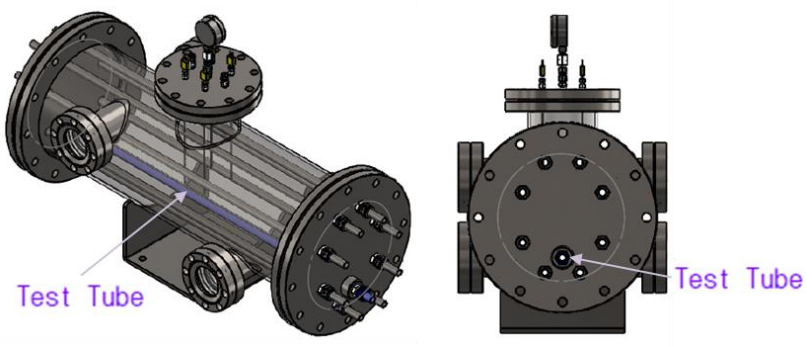

Fig. 1. Schematic drawing of test chamber and test tube.

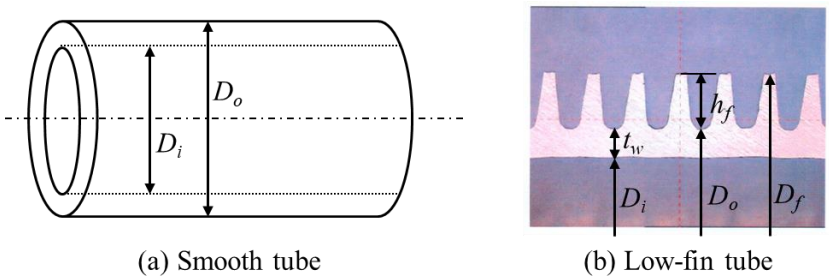

Fig. 2. Designation of geometric parameters for smooth and low-fin (enhanced) tubes.

Table 1. Geometric parameters of smooth and low-fin tubes

	D_i (mm)	D_o (mm)	t_w (mm)	D_f (mm)	h_f (mm)
Smooth tube	13.39	15.87	1.24	-	-
Low-fin tube	11.81	13.07	0.63	15.73	1.33

The chamber temperature was maintained using eight tubes embedded in the chamber, where water and ethylene glycol mixture flows. Four tubes are in the vapor region of the chamber and utilized to condense the ammonia vapor generated from the test tube. The remaining four tubes are located at the liquid region of the chamber and employed to maintain the saturation temperature of the liquid pool of ammonia. The liquid temperature of the ammonia pool was measured at two points using T-type thermocouples, and the internal pressure of the chamber was acquired from the pressure transducer. The temperature of the test tube was controlled by circulating hot distilled water through the tube. Inlet and outlet temperatures of the test tube were measured with precise RTD sensors with 1/10 DIN accuracy (±0.03 ℃ tolerance at 0 ℃). The hot distilled water was circulated by a gear pump and the flow rate was measured with Coriolis mass flowmeter. The flow rate through the test tube was maintained to be 3.8 kg/min over the entire tests. Two reinforced glass windows were equipped at the top and bottom regions of the chamber to observe the boiling and condensation phenomena at the liquid and vapor regions, respectively. A high-speed camera with a frame rate of 2,000 fps was utilized for capturing the bubble nucleation on the heated tube. The entire test chamber was thermally insulated with fiberglass insulation tapes having low thermal conductivity of 0.05 W/mK.

2.2. Experimental procedure and data reduction

Ammonia is filled into the test chamber in the following procedure. The internal pressure of the test chamber is lowered down to the absolute pressure of 3–5 mTorr using a rotary vacuum pump. Once the non-condensable gas is completely extracted from the chamber, the valve to the vacuum pump is closed. Then, the valve to the ammonia cylinder is open, and the liquid ammonia is injected into the chamber. When the liquid level of ammonia gets to the center of the chamber, the valve is closed to finish the filling process. The boiling experiment was conducted at three saturation pressures of 6.15, 8.57, and 11.7 bar, which correspond to the saturation temperatures of 10, 20, and 30 ℃, respectively. Once the internal temperature and pressure are maintained at the designated saturation temperature and pressure using eight temperature control tubes, the hot water begins to flow through the test tube. At the initial step, hot water temperature is merely 2.5 K higher than the saturation temperature of ammonia pool. Once the inlet and outlet temperatures of the test tube reach steady state, all data including temperature, pressure and flow rate are stored for 10 min, and the hot water temperature is increased to the next level stepwise.

Evaporation or boiling heat transfer rate, Q is obtained from the following energy balance equation.

$$Q = \dot{m} c_p \Delta T = \dot{m} c_p (T_i - T_o) \tag{1}$$

T_i and T_o refer to the inlet and outlet water temperature of the test tube, respectively. The heat transfer rate, Q is also expressed as multiplying overall heat conductance and log-mean temperature difference as shown in Eq. (2).

$$Q = UA\Delta T_{lm} \tag{2}$$

The LMTD (log-mean temperature difference) is defined as,

$$\Delta T_{lm} = \frac{\Delta T_i - \Delta T_o}{ln(\Delta T_i / \Delta T_o)} \tag{3}$$

$$\text{here,} \quad \Delta T_i = T_i - T_\infty, \ \Delta T_o = T_o - T_\infty$$

T_∞ refers to the liquid pool temperature surrounding the test tube. Boiling heat transfer coefficient, h_b can be acquired from the following thermal resistance relation.

$$\frac{1}{UA} = \frac{1}{h_i A_i} + \frac{ln(D_o/D_i)}{2\pi kL} + \frac{1}{h_b A_o} \tag{4}$$

Total thermal resistance comprises thermal resistance of internal convection, conduction thermal resistance through the tube wall, and thermal resistance of boiling heat transfer. Convective heat transfer coefficient of internal water flow through the test tube was obtained from the Gnielinski correlation [13].

$$Nu_D = \frac{(f/8)(Re_D - 1000)Pr}{1+12.7(f/8)^{1/2}\left(Pr^{2/3}-1\right)} \tag{5}$$

$$0.5 \le Pr \le 2000, \quad 3000 \le Re_D \le 5 \times 10^6$$

Since Reynolds numbers in the present study range from 5,282 to 14,531, the correlation is applicable to obtain the internal convective heat transfer coefficient. Then, boiling heat transfer coefficient (h_b), the remaining unknown in Eq. (4), can be acquired. The average wall temperature on the test tube is calculated in the following equation.

$$\overline{T_w} = (T_i + T_o)/2 + Q \times \left(\frac{1}{h_i A_i} + \frac{ln(D_o/D_i)}{2\pi kL}\right) \tag{6}$$

2.3. Uncertainty analysis

T-type thermocouple employed to measure the liquid pool temperature has an uncertainty of ±0.5 ℃. 1/10 DIN-class RTDs to measure inlet and outlet temperatures of the test tube are extremely accurate with an uncertainty of ±0.03 ℃ at 0 ℃. The uncertainty increases with temperature according to the following relation.

$$U(T) = (0.3 + 0.0005 \times T)/10 \tag{7}$$

where, T is measured temperature in ℃. The resultant uncertainty of LMTD (log mean temperature difference) are calculated to be from 1.9% to 14.4%. The mass flowmeter has an uncertainty of ±0.1%, and the pressure transducer has an accuracy of ±0.08%, both of which are provided by manufacturers. As a result, the uncertainty of obtained heat transfer rates ranges from 1.1% to 20.5%, and the uncertainty of boiling heat transfer coefficients is 16.1% in average.

3. Results and Discussion

3.1. Hysteresis in boiling curve

Figure 3(a) exhibits the boiling curve on the smooth tube in the ammonia pool at the saturation temperature of 30 ℃ corresponding to the saturation pressure of 11.7 bar. It is noticeable that there is discrepancy between boiling curves with increasing heat flux and decreasing heat flux. In case the heat flux is increased from low to high, bubble generation is observed only in some areas of the tube until the heat flux

reaches 11,000 W/m^2. It seems that boiling incipience is delayed until the superheat is large enough to sustain the bubble generation. The large superheat required to generate the bubble is attributed to the superior wettability of ammonia on the stainless steel surface owing to the small surface energy. Ammonia is highly wettable on most of metal surfaces, resulting in the low contact angle less than 10°. The low contact angle is responsible for the suppression of bubble nucleation because it decreases the initial radius of the vapor embryo. The small initial radius of the embryo results in the increase of the wall superheat for attaining bubble nucleation. In contrast, in case the heat flux decreases from high to low, nucleate boiling is preserved over the entire tube surface even at the low heat fluxes less than 10,000 W/m^2. The bubble generation is facilitated at the low heat flux because the remaining vapor after the departure is large enough to keep the bubble generation at the low wall superheat. Boiling heat transfer coefficients at two cases show maximum 46% difference near the heat flux of 7,800 W/m^2 as shown in Fig. 3(b). Since the large hysteresis leads to different heat transfer performance according to the heating and cooling paths, consistent operation of actual heat exchangers might be threatened. In real heat transfer applications, it is greatly important to minimize the hysteresis by using surface modification techniques such as wettability control or porous structures.

Figure 4 shows different boiling phenomena at the heat flux near 11,000 W/m^2 for both increasing and decreasing heat flux cases. At the increasing case, only a few bubbles can be seen at the low heat flux. In contrast, numerous bubbles are observed over the entire tube surface at the decreasing case. Certainly, the increased number of bubble nucleation is responsible for improvement of heat transfer performance at the decreasing case as shown in Fig. 3.

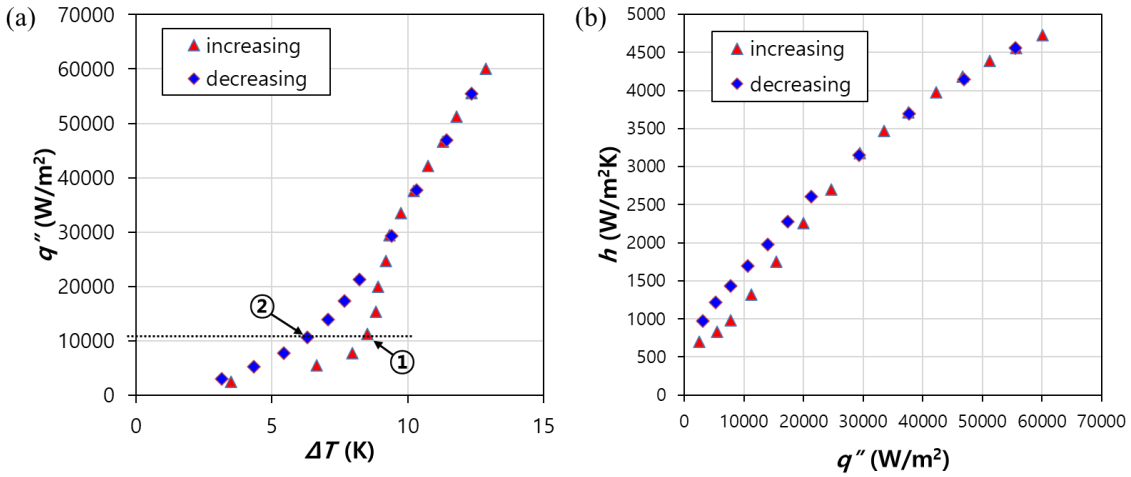

Fig. 3. Hysteresis in pool boiling of ammonia, (a) boiling curve and (b) heat transfer coefficient at P_{sat} = 11.7 bar.

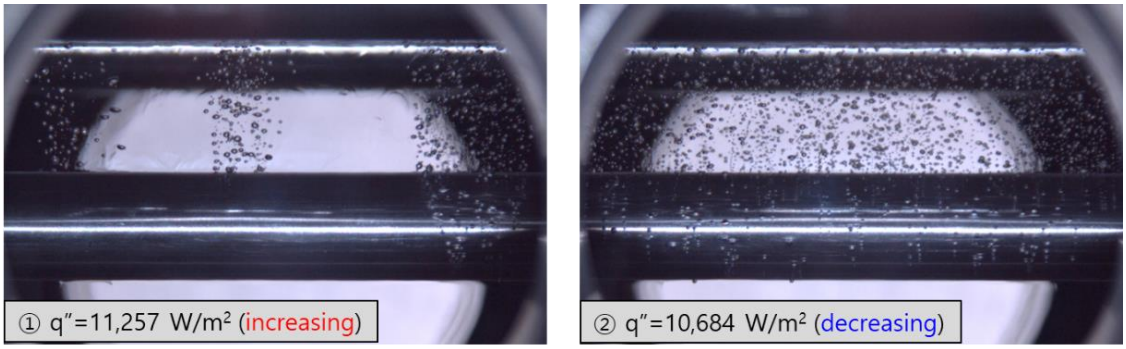

Fig. 4. Bubble nucleation comparison in increasing q'' and decreasing q'' cases at P_{sat} = 11.7 bar.

3.2. Effect of saturation pressure

With increasing the saturation pressure in the ammonia pool, thermodynamic properties such as liquid density, vapor density, surface tension, and heat of vaporization are changed. Since the variation of thermodynamic properties affect the boiling heat transfer performance, heat transfer coefficients at three different saturation pressure from 6.15 bar (T_{sat} = 10 ℃) to 11.7 bar (T_{sat} = 30 ℃) were compared as shown in Fig. 5. As the saturation pressure increases, boiling curves move to the left, implying that the boiling heat transfer is enhanced. It is known that bubble departure diameter decreases with increasing the saturation pressure owing to the variation of thermodynamic properties. Eq. (8) shows the correlation about the bubble departure diameter proposed by Cole [14].

$$Bo^{1/2} = 0.04Ja \tag{8}$$

$$\text{here,} \quad Bo = \frac{g(\rho_l - \rho_v){d_d}^2}{\sigma}, \quad Ja = \frac{\rho_l c_{pl}(T_w - T_{sat})}{\rho_v h_{lv}}$$

where, d_d refers to the bubble departure diameter. The bubble departure diameters of ammonia at the wall superheat of 7 ℃ are calculated to be 1.21, 1.08, and 0.97 mm at three different saturation pressures. Figure 6 clearly shows that the bubble departure diameter increases with increasing the saturation pressure. On the contrary, number of nucleation sites and departure frequency are increased with increasing the saturation pressure. More bubble nucleation sites at higher saturation pressure are also revealed in the captured images in Fig. 6.

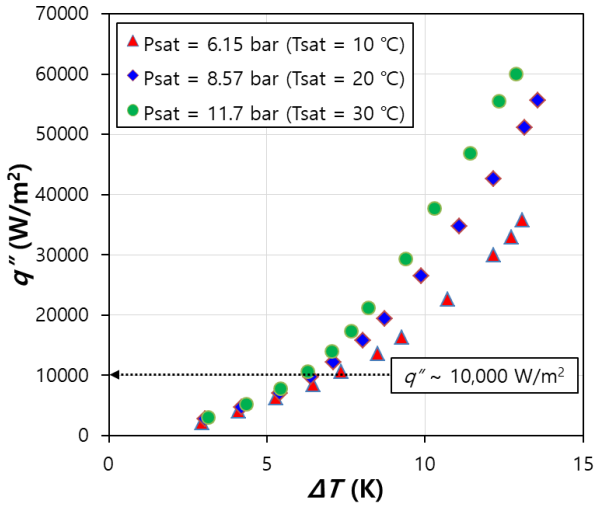

Fig. 5. Boiling curves according to the saturation pressure from 6.15 to 11.7 bar (decreasing q'').

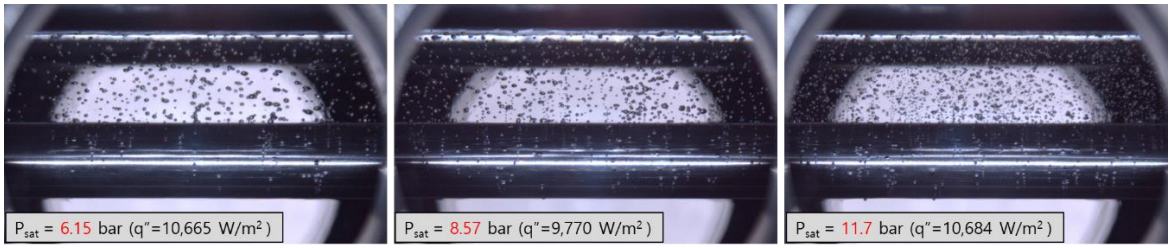

Fig. 6. Comparison of bubble nucleation according to the saturation pressure from 6.15 to 11.7 bar (decreasing q'').

3.3. Comparison with previous correlations

The present data are compared with previous correlations about pool boiling heat transfer coefficients on the smooth tube. Following four correlations (Mostinski [15], Gorenflo [16], Rohsenow [17], and Stephan-Abdelsalam [18]) were selected for comparison.

$$h_b = 0.1011(P_c)^{0.69} q^{0.7} \left[1.8\left(\frac{P}{P_c}\right)^{0.17} + 4\left(\frac{P}{P_c}\right)^{1.2} + 10\left(\frac{P}{P_c}\right)^{10}\right] \quad \text{(Mostinski)} \tag{9}$$

$$h_b = h_0 \left(\frac{q}{q_0}\right)^{n(P_r)} F(P_r) \left(\frac{R_a}{R_{a0}}\right)^{0.133} \quad \text{(Gorenflo)} \tag{10}$$

$$h_b = \frac{1}{C_{sf}} \frac{C_{pl}}{h_{fg}^{0.67}} \left[\frac{1}{\mu_l}\sqrt{\frac{\sigma}{g(\rho_l - \rho_v)}}\right]^{-0.33} (q)^{0.67} (Pr_l)^{-1.7} \quad \text{(Rohsenow)} \tag{11}$$

$$\frac{h_b D_b}{k_l} = 207 \left(\frac{q D_b}{k_l T_{sat}}\right)^{0.745} \left(\frac{\rho_v}{\rho_l}\right)^{0.581} (Pr_l)^{0.533} \quad \text{(Stephan-Abdelsalam)} \tag{12}$$

Gorenflo and Rohsenow's correlations exhibit relatively high heat transfer coefficients (upper bound), and Stephan-Abdelsalam correlation provides lower heat transfer coefficients (lower bound). The present data in case of increasing heat flux shows good agreement with the Stephan-Abdelsalam correlation, and the data in the decreasing case are somewhat higher than the Stephan-Abdelsalam correlation, and approach the Mostinski correlation, especially at the low heat flux region. The following empirical relations are deduced for the pool boiling heat transfer of ammonia at the saturation temperature of 30 ℃.

$$h = 0.9168(q'')^{0.7846} \quad \text{(increasing } q'') \tag{13}$$

$$h = 10.472(q'')^{0.5542} \quad \text{(decreasing } q'') \tag{14}$$

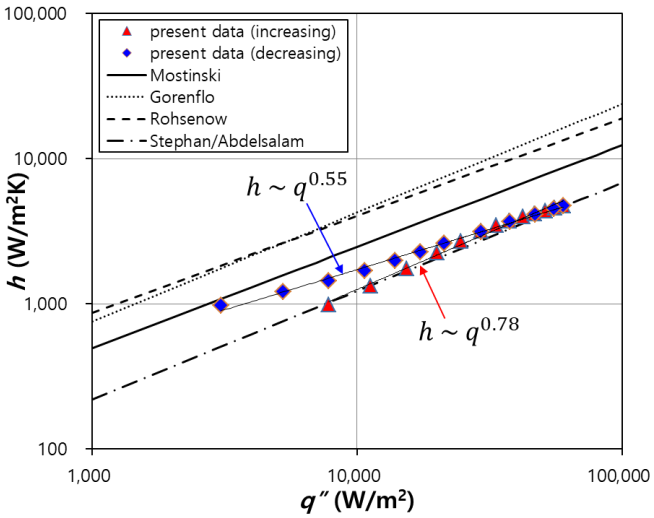

Fig. 7. Comparison with previous correlations at the saturation pressure of 11.7 bar.

3.4. Smooth tube vs. Low-fin tube

The low-fin tube has an outer diameter (D_o) of 13.07 mm as indicated in Fig. 2 and Table 1. The heat transfer coefficient, h_b, is calculated from the tube surface area based on the outer diameter. Total heat transfer rate (Q) is obtained from the following equation.

$$Q = h_b A_o \Delta T_w \tag{15}$$

Figure 8 shows boiling curve and boiling heat transfer coefficient on the low-fin tube compared with those on the smooth tube at the saturation pressure of 11.7 bar. It is noticeable that boiling hysteresis is enlarged on the low-fin tube compared with the smooth tube. The enlarged hysteresis resulted from the decrease in wall superheat on the finned surface compared with that on the smooth tube because there is temperature gradient along the fin height. Despite the hysteresis, the low-fin tube exhibits higher heat transfer coefficients in both increasing and decreasing heat flux cases. The heat transfer coefficient (h_b) increased by 61% in increasing q'' case and by 111% in decreasing q'' case.

Since the heat transfer area is varied, thermal performance of the low-fin tube can be compared with that of the smooth tube based on the thermal conductance which is defined as multiplying heat transfer coefficient and heat transfer area, h_bA_o. Figure 9 shows the thermal conductance of the low-fin tubes normalized with that of the smooth tube in increasing and decreasing heat flux cases. It is concluded that the boiling heat transfer on the low-fin tube is enhanced by 33% (increasing q'') and 74% (decreasing q'') over the smooth tube.

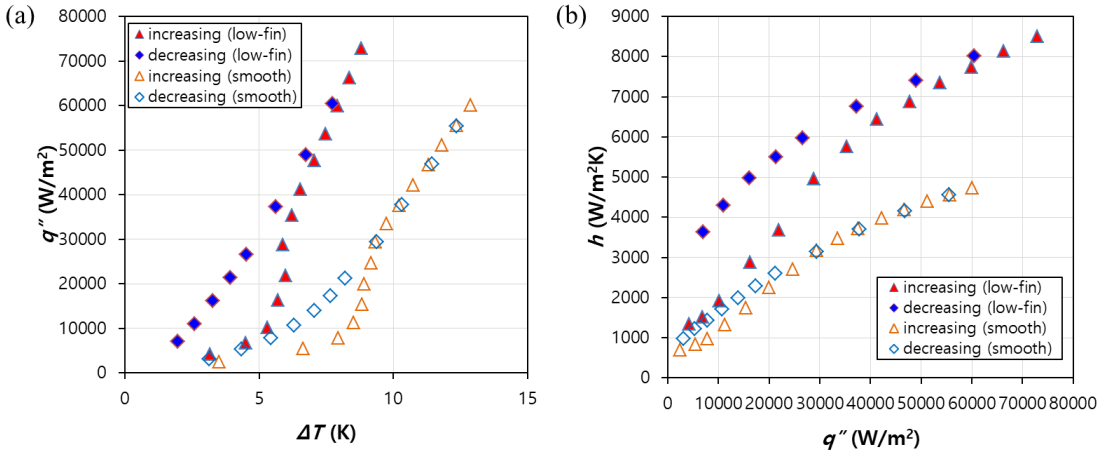

Fig. 8. Effect of enhanced structure (low fins) on boiling heat transfer of ammonia.

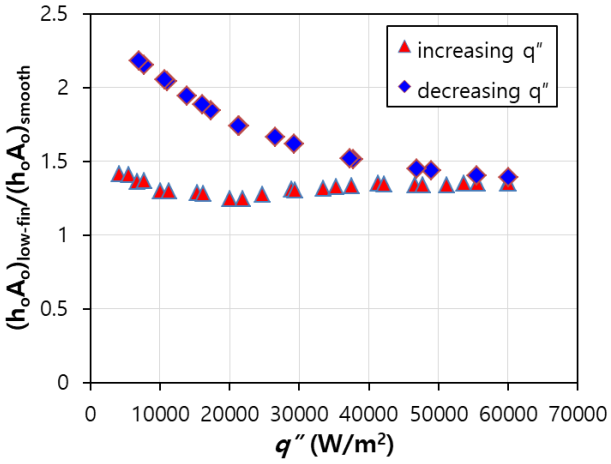

Fig. 9. Thermal conductance of the low-fin tube compared with the smooth tube.

4. Conclusion

Boiling heat transfer of ammonia was investigated in a flooded evaporator for an adsorption heat pump at the saturation pressures of 6.15, 8.57, and 11.7 bar. Large hysteresis between increasing heat flux case and decreasing heat flux case was observed in the boiling curves, which is ascribed to the low surface energy of ammonia. Higher heat transfer coefficients were obtained with increasing saturation pressure, and the measured heat transfer coefficients were best matched with the previous Stephan-Abdelsalam's correlation. Since the enhanced tube with low fins exhibited 33% (increasing q'') and 74% (decreasing q'') higher heat transfer performance compared with those on the smooth tube, employing the low-fin tubes in a flooded evaporator is expected to augment thermal performance of the adsorption heat pump system.

Acknowledgements

This work was supported by Korea Institute of Energy Technology Evaluation and Planning (KETEP) and the Ministry of Trade, Industry & Energy (MOTIE) of the Republic of Korea. (Grant No. 20212050100010).

References

[1] Yang Z, Qu M, Gluesenkamp KR. Ammonia-based chemisorption heat pumps for cold-climate heating applications: A comprehensive review. *Appl Therm Eng* 2020;**179**:115674.
[2] Dias JM, Costa VA. Adsorption heat pumps for heating applications: A review of current state, literature gaps and development challenges. *Renewable Sustainable Energy Rev* 2018;**98**:317-327.
[3] Spindler K. Overview and discussion on pool boiling heat transfer data and correlations of ammonia. *Int J Refrig* 2010;**33.7**:1292-1306.
[4] Arima H, Monde M, Mitsutake Y. Heat transfer in pool boiling of ammonia/water mixture. *Heat Mass Transf* 2003;**39.7**:535-543.
[5] Danilova GN, Dyundin VA, Borishanskaya AV, Soloviyov AG, Kozyrev AA. Effect of surface conditions on boiling heat transfer of refrigerants in shell-and-tube evaporators. *Heat Transf-Soviet Res* 1990;**22.1**:56-65.
[6] Djundin VA, Solov′ev AG, Borisanskaja AV, Vol′nych J. Influence of the type of surface on heat transfer in boiling. *Kholod Tekh* 1984;**5**:33-37..
[7] Ayub ZH, Chyu MC, Ayub AH. Different types of carbon steel enhanced tubes in ammonia flooded evaporator. *Heat transf eng* 2006;**27.5**:39-44..
[8] Zeng X, Chyu MC, Ayub ZH. Experimental investigation on ammonia spray evaporator with triangular-pitch plain-tube bundle, Part I: tube bundle effect. *Int J Heat Mass Transf* 2001;**44.12**:2299-2310..
[9] Zheng JX, Jin GP, Chyu MC, Ayub ZH. Flooded boiling of ammonia with miscible oil outside a horizontal plain tube. *HVAC&R Res* 2001;**7.2**:185-204..
[10] Abbas A, Ayub ZH, Khan TS, Ayub AH, Chattha JA. A Review of Correlations for Outside Boiling of Ammonia on Sinrgle Tube and Bundles. *Heat Transf Eng* 2018;**39.16**:1425-1436.
[11] Fernández-Seara J, Pardiñas ÁA, Diz R. Experimental heat transfer coefficients of pool boiling and spray evaporation of ammonia on a horizontal plain tube. *Int J Refrig* 2016;**67**:259-270.
[12] Fernández-Seara J, Pardiñas ÁÁ, Diz R. Heat transfer enhancement of ammonia pool boiling with an integral-fin tube. *Int J Refrig* 2016:**69**:175-185..
[13] Gnielinski V. New equations for heat and mass transfer in turbulent pipe and channel flow. *Int Chem Eng* 1976;**16.2**:359-368..
[14] Cole R. Bubble frequencies and departure volumes at subatmospheric pressures. *AIChE J* 1967;**13.4**:779-783..
[15] Mostinski IL. Application of the rule of corresponding states for calculation of heat transfer and critical heat flux. *Teploenergetika* 1963;**4.4**:66-71..
[16] Gorenflo D. *VDI Heat Atlas*. VDI-Verlag GmbH, Dusseldorf, Germany: Springer; 1993.
[17] Rohsenow WM. A method of correlating heat-transfer data for surface boiling of liquids. *Trans Am Soc Mech Eng* 1952;**74.6**:969-975..
[18] Stephan K, Abdelsalam M. Heat-transfer correlations for natural convection boiling. *Int J Heat Mass Transf* 1980;**23.1**:73-87..